

Chapter 8

Biological Nanoparticles: Optical and Photothermal Properties

Aditya Saran, Rajender Boddula, and Sharda Ranjan Sharan

Abstract The synthesis of metal nanoparticles (NPs) through biological approach has proved to be safer than chemical approach and environment friendly. Still the quality of the biologically synthesized metal NPs could not touch the quality standard of chemically synthesized metal NPs. This limits the application of biologically synthesized NPs. In the biosynthetic approach, the complications lie in complicated biochemical pathways, cellular morphology, physiology and other biological and environmental limitations. On the other hand, chemical synthesis process is simple because of limited chemical reactions and has ease to control and change the required physical and chemical parameters like pH, temperature, humidity, etc. as per need. Thus, chemically synthesized NPs are more uniform in shape and size, have defined surface modification and are stable than its biological counterpart. Here we will focus on the limitations of biological synthesis of metal NPs through fungus and discuss the various approaches to counter these limitations to enhance the quality of metal NPs so that biologically synthesized NPs can be used practically on a wider scale.

A. Saran (✉)

ORCID ID: 0000-0001-5433-8769; CAS Key Laboratory of Standardization and Measurement for Nanotechnology, National Center for Nanoscience and Technology, No.11 ZhongguancunBeiyitiao, Beijing 100190, People's Republic of China
e-mail: aditya8march@yahoo.com; aditya8march@gmail.com

R. Boddula

ORCID ID: 0000-0001-8533-3338; CAS Key Laboratory for Nanosystem and Hierarchical Fabrication, National Center for Nanoscience and Technology, No.11 ZhongguancunBeiyitiao, Beijing 100190, People's Republic of China

S.R. Sharan

Department of Physics, Deoghar College, S K M University, Dumka 814101, India

8.1 Introduction: Nanoparticles, Nanostructures and Nanomaterials

Nanotechnology deals with various structures of matter having dimensions of the order of a 10^{-9} of a metre. Nanoparticles are generally considered to be a number of atoms or molecules bonded together with a radius of <100 nm. The structure which comes under the dimension of a nanometre is also considered as nanostructures. Hence, a haem molecule which is incorporated into haemoglobin molecule can be considered as nanoparticle, and most of the viruses are nanostructures. Thus nanoparticles and nanostructures can be built by assembling individual atoms or subdividing bulk materials.

The physical and chemical properties change at dimensions of nanometre scale. Mostly the crystal structure of large-sized nanoparticles remains the same as that of its bulk, but lengths of primitives are somewhat different. It has been verified from X-ray diffraction experiment that 80 nm aluminium particle has face-centred cubic (fcc), which the bulk aluminium has. Particles of sizes smaller than 5 nm may have different structures. Three to 5 nm gold particles have an icosahedral structure, whereas its bulk has fcc structure. If one geometrical dimension has a nanosize length, the structure is called a quantum well. If the electronic structure is quite different from the arrangement where two dimensions in three-dimension are of nanometre length, it is called a quantum wire. But if all the lengths in all three geometrical dimensions are in the nano-range, then it is called a quantum dot (Poole and Owens 2003).

Nanomaterials are made up of cluster of atoms which can be assumed as superatoms (Khanna and Jena 1995). The number of atoms which makes the cluster stable is called as structural magic number (Poole and Owens 2003). In an atom the positive charge of the nucleus is localized at a point and the electrons respond to $1/r$ potential. On the other hand, in a cluster, the positive charge is assumed to be distributed over a positive ion core of the size of the cluster, and the electrons respond to a square-well-type potential that is attractive to the core. The electron energy levels in clusters are discrete and can be labelled by principal and angular momentum quantum numbers, but the ordering of levels is different from electron's energy levels in an atom. The electronic structure of an atom is like $1s^2, 2s^2, 2p^6, 3s^2, 3p^6, 3d^{10}, 4s^2$ and so on, but in case of cluster, it is changed to $1s^2, 1p^6, 1d^{10}, 2s^2, 1f^{14}, 2p^6$ and so on. For example, electronic structure of aluminium is $1s^2, 2s^2, 2p^6$ and $3s^1$. Since Al is trivalent, an Al_{13} cluster has 39 electrons, which, in a jellium picture, would correspond to an electronic configuration of $1s^2, 1p^6, 1d^{10}, 2s^2, 1f^{14}$ and $2p^5$. Note that chemical property is determined by the electrons in the outermost orbit. Cluster also has the similar electronic features in ionization potential, electron affinity and reactivity, but uniquely their nuclear potential is fixed, and attractive potential can be easily modulated. The attractive potential can be modulated by changing its composition, the range can be controlled by its size, and its shape can be controlled by the overall topology. Further, the electronic nature can be controlled by

manipulating the number of valence electrons by doping with foreign atoms, and the nature of the electronic degeneracy can be controlled by changing the geometry. This allows much better control of the electronic spectrum and thereby on its properties (Rao et al. 1999). This is the reason why nanomaterial shows different properties from its bulk material (Fig. 8.1).

8.2 Metal Nanoparticles

This chapter deals with metal nanoparticles which may or may not be nanomaterials. The optical and photothermal properties of metallic nanoparticle are mainly dependent upon its size and surface area. The nobility of a metal is decided by the ability of metal surface to be oxidized. Gold is the only metal which has endothermic chemisorption energy. It means that it will not make bond to oxygen at all, and hence, it remains inert in an oxygen atmosphere. The d-state orbital of Au is so low in energy that the interaction with oxygen 2p states is net repulsive. So it is unlikely that Au should be a good catalyst for an oxidation reaction. Uniquely in oxidation

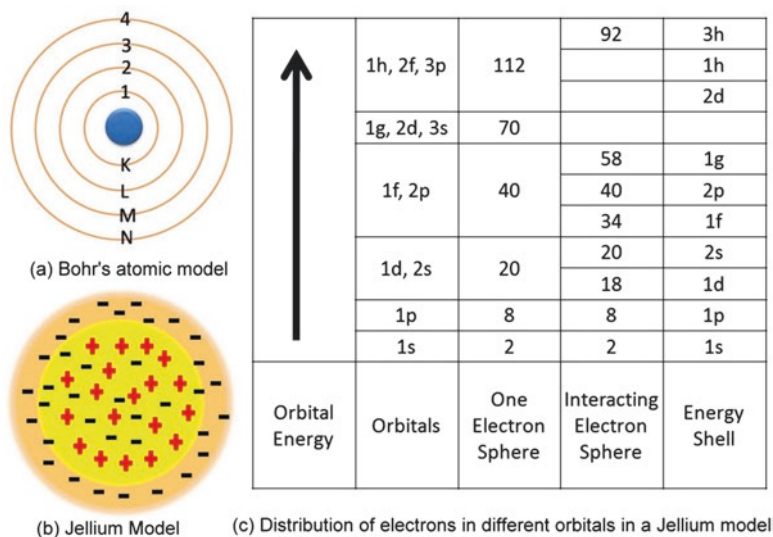


Fig. 8.1 A comparison between Bohr's atomic model and jellium model; (a) Bohr's atomic model; (b) positive charge is assumed to be distributed over a positive ion core of the size of the cluster, and the electrons respond to a square-well-type potential that is attractive within the ion core and zero outside, shown in jellium model; (c) distribution of electrons in different orbitals in a jellium model

of CO, Au nanoparticles are very good catalyst even at room temperature. This activity of Au nanoparticle depends upon the size (Au <5 nm shows catalytic activity) (Hvolbæk et al. 2007).

8.3 Excitation and Relaxation Processes of Metal Nanoparticles

Generally an excitation due to intersystem crossing, internal conversions, fluorescence, etc. has a defined time scale for the average lifetime of an excited state (Turro et al. 2012). In the case of metals, which have a relatively high number of electrons close in energy to a large number of available empty states, their electrons can freely transfer between states at room temperature. So in these cases, the time scale for excitation is not limited (Hartland 2011). As per Mie theory, the choice of metal, as well as size, shape, surrounding matrix, surface-bound molecules and degree of aggregation of the particles, determines the frequency of light that can excite plasmons (Kelly et al. 2003; Stamplecoskie and Scaiano 2010). Light is an electromagnetic wave and has both sinusoidal electric and magnetic fields mutually transverse and always in phase, and these are transverse to the direction of propagation of light wave. When light of a suitable wavelength or frequency is made incident on the surface of the metal, the electric field in the incident light ray exerts force on electrons and thus causes their displacements and hence changes the volume density of electron, i.e. number of electrons per unit volume. Electric field of light expends energy, that is, light loses its intensity and it is absorbed. A periodic fluctuation of positive and negative charges occurs which is called 'surface plasmon polaritons'. The nuclei being heavy provide a restoring force on the dynamic lighter electrons which have moved away. This is similar to plasma oscillations in physics. The oscillating charges create electromagnetic radiation.

For this reason, the frequency that can be used to excite plasmon absorptions is a function of both the metal and the dielectric medium surrounding it. Some electrons of metal nanoparticles get instantaneous excitation due to incident light. Moreover the surface curvature is not uniform with respect to wavelength of light. For this reason, the plasmon absorptions by nanoparticles occur in the visible region of the electromagnetic spectrum, giving rise to the multitude of colours displayed by metal nanoparticles. The plasmons of nanoparticles cannot move away because of their confinement to the particle. Hence they are called as localized surface plasmons (LSP).

Kasha's rule states that the rate of an electronic relaxation is inversely proportional to the difference in energy between energy states. This means that, for metals with overlapping filled and unfilled energy bands, the rate of relaxation must be very fast. The coherent oscillating electrons collide with one another causing the electrons to rapidly go out of phase with one another. This dissimilarity in electron phases causes a non-Fermi distribution of electrons, and it occurs within the ~10 fs

of excitation. The excited electrons further scatter with each other leading to a more random or chaotic distribution. The ‘electron-electron’ scattering occurs within the first ~ 100 fs after excitation. Most spectroscopic techniques use lasers with greater than 100 fs pulse widths, so these first electron relaxation steps are very rarely observed experimentally. The final process in plasmon relaxation dissipates heat to its surrounding. The heat transfer depends upon the excitation and thermal conductivity of the medium. Heat transfer to the surroundings occurs in hundreds of picoseconds to nanoseconds, following excitation. The ability to absorb a lot of light, and release that energy locally in a short amount of time (< 1 ns), is a unique property of metal nanoparticles (Alarcon et al. 2015).

8.4 Plasmonics and Surface Plasmon Resonance

Plasmonics is a phenomenon of electromagnetic resonance encountered in nanostructured metals, due to collective oscillation of conduction electrons called plasmons. Under certain conditions plasmons are excited by light that leads to strong light scattering, absorption and local electromagnetic field (Fig. 8.2). The effect can be manipulated by doing alteration and changes in the defined conditions (Fu et al. 2012). At nanoscale we are in the middle between classical and quantum effects, macroscopic and microscopic properties of the matter (Wolf 2015).

The phenomenon of surface plasmon resonance (SPR) was first observed by Wood in 1902. He made polarized light incident on a reflection grating which causes final diffraction of light producing a pattern of ‘anomalous’ dark and light bands

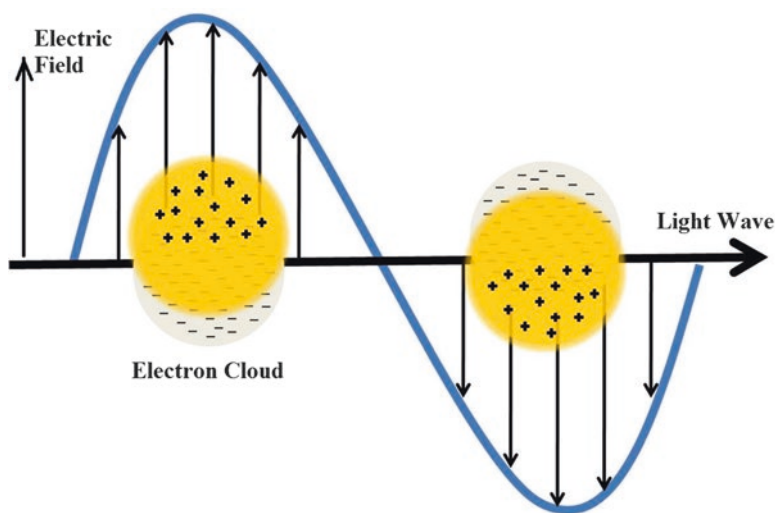


Fig. 8.2 Schematic illustration of plasmon excitation causing an instantaneous collective oscillation of electrons

(Wood 1902, 1912). Lord Rayleigh initiated the physical interpretation of this phenomenon (Rayleigh 1907), which was further refined by Fano (1941). Finally a detailed explanation came in 1968 by Otto (1968) and independently by Kretschmann and Raether (1968).

Experimentally a dip in the intensity of the reflected light is observed when a polarized light is incident from the light source on the sensor chip with a gold coating on a prism. At a certain angle of incidence (ϕ), excitation of surface plasmons occurs which results in a dip in the intensity of the reflected light. This dip in intensity is caused by the oscillation of the free electrons which is generated because of the interaction of photons of plane-polarized light with the free electrons of the metal layer. The angle at which the maximum loss of the reflected light intensity occurs is called resonance angle or SPR angle. The SPR angle is dependent on the optical characteristics of the system such as on the refractive indices of the media at both sides of the metal, usually gold. When an accumulated mass adsorbs (protein, DNA, etc.) on the surface of metal in its vicinity and refractive index at the prism side remains constant, the surface plasmon resonance condition changes, and the shift of SPR angle provides the information on kinetics.

8.4.1 SPR Assay

To construct a SPR assay, the surface of the sensor needs to be modified to allow selective capturing and thus selective measurement of the target compound. Often SPR measurements are carried out to determine the kinetics of a binding process. Recently SPR signals are also utilized in the detection of biomolecules through ELISA (de la Rica and Stevens 2012, 2013; Rodriguez-Lorenzo et al. 2012; Cecchin et al. 2014; Nie et al. 2014; Peng et al. 2014; Xianyu et al. 2014; Liang et al. 2015; Zhang et al. 2015; Huang et al. 2016; Zhao et al. 2016; Hu et al. 2014).

8.4.2 Surface Plasmon Resonance (SPR) Biosensors

The term biosensor was introduced around 1975. Literally all devices capable of reporting parameters of the living body are biosensors including a thermometer. As per present definition, a biosensor should have a recognition element comprised of biological origin and a physiochemical transducer.

The transducer detects a physiochemical change because of specific interaction between the target analyte and the biological material. Further the transducer then yields an analogue electronic signal proportional to the concentration of a specific analyte/analytes. Application of SPR-based sensors to biomolecular interaction monitoring was first demonstrated as physical methods for label-free, real-time detection of biomolecules by Lundstrom in 1983 (Liedberg et al. 1983). In 1990, Pharmacia Biosensor AB launched the first commercial SPR product, the Biacore

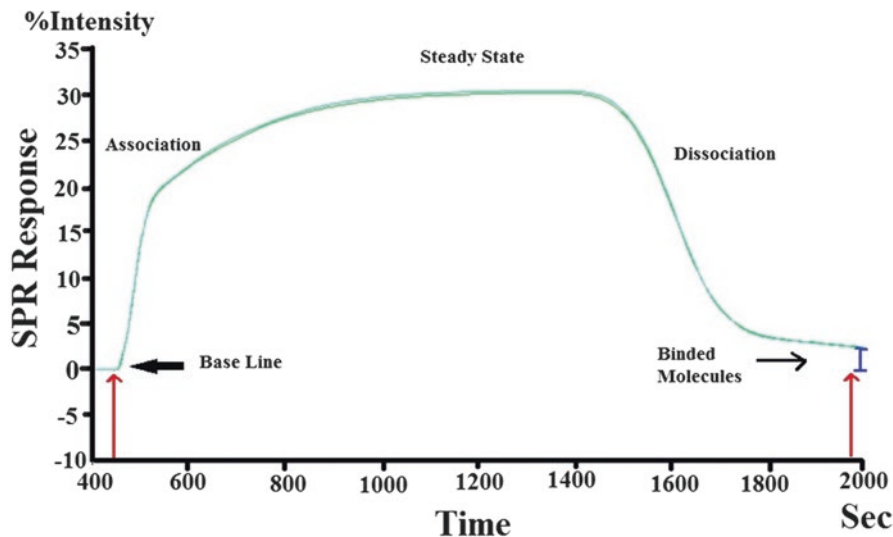


Fig. 8.3 A typical SPR signal of SPR biosensor detecting the binding of N-succinimidyl 3-(2-pyridylidithio)propionate (SPDP) to human immunoglobulin G (IgG). The red arrow is showing the baseline of human IgG. The X-axis is showing the time line in seconds for the association, steady state and dissociation of SPDP molecule. The blue bar is the SPR response in terms of intensity for SPDP molecule. Higher SPR response corresponds to higher binding

instrument, which was the most advanced, sensitive, accurate, reliable and reproducible direct biosensor technique (Jonsson et al. 1991). A typical binding of SPDP to human IgG is demonstrated and analysed by SPR as shown in Fig. 8.3.

8.5 Surface-Enhanced Raman Spectroscopy (SERS)

Raman spectra usually contain many sharp peaks that correspond to specific molecular vibrational frequencies, and these can provide a clear signature defining the presence of specific molecules in a sample. Accordingly, Raman spectra can be used to qualitatively and quantitatively discriminate between chemical species in materials (Motz et al. 2006).

Raman scattering is an inelastic phenomenon that occurs when a sample is illuminated by a laser light, as first demonstrated by Raman and Krishnan in 1928 (Raman and Krishnan 1998). In Raman scattering the frequency or wavelength of scattered light remains mostly unchanged except very weak lines with increase or decrease in wavelength. This increase in wavelength is Stokes Raman scattering, and decrease in wavelength is anti-Stokes Raman scattering.

The signals are weak and to enhance it, high-power lasers and long acquisition times are required which are unsuitable for biological samples. In order to enhance

the intensity of Raman spectral lines, a widely used method is SERS. Finally Fleischmann in 1974 (Fleischmann et al. 1974) observed the reliability on absorption effect on Raman spectral lines. The absorption function of analyte(s) relies on the surface of metal structures. The intensity of absorbed Raman lines can be 106–108 times more. This is indicative of the importance of SERS. It is being discussed in the following section.

Surface-enhanced Raman scattering (SERS) bypasses this limitation (Alarcon et al. 2015). SERS evolves as the most promising label-free technique for molecular sensing (Campion and Kambhampati 1998). SERS, used for extremely low concentrations of molecules, overcome the low Raman cross-sectional barrier by exploiting the large field enhancement caused by electromagnetic coupling between the nanoparticles (Alarcon et al. 2015). Under such conditions, the Raman signal of the target molecule is enhanced by several orders of magnitude, enabling detection down to a single molecule (Qian and Nie 2008; Abalde-Cela et al. 2010; Oh et al. 2011; Choi et al. 2010). Generally SERS is performed on gold, silver and copper. The absorbance is mainly in the visible and near-IR wavelengths. Raman signal is amplified because of two reasons: (1) the strong enhancement of the electromagnetic field by the localized surface plasmon resonance (SPR) of metallic nanostructures and (2) surface chemical enhancement mechanism (Schatz and Van Duyne 2002; Faulds et al. 2004).

SERS has been widely used as an analytical technique in the fields of biochemistry, forensics, food safety, threat detection and medical diagnostics (Qian and Nie 2008; Ewená Smith 2002; McNay et al. 2011; Graham and Goodacre 2008). The reason behind the wide acceptance of SERS is that it is a label-free molecular fingerprint down to the level of single-molecule detection with multiplex detection which works in both in situ and in vitro detection with minimum sample requirements (Alarcon et al. 2015; Siddhanta et al. 2017).

8.6 Photothermal Effect

Photothermal therapy using metal nanoparticles exploits the infrared light to heat conversion of metal nanoparticles for selective destruction of tumours. The larger wavelength has longer penetrating depth than the shorter wavelength; this is the reason some of the red light makes it through the skin or mouth tissue. In photothermal therapy, the wavelength of excitation is an important factor then, since only red light can penetrate deep into the tissue to excite the absorbing species (that subsequently releases heat). The multiphoton cross section for metal nanoparticles is very high in comparison to dyes. This becomes even more relevant in PPTT treatments when it is desirable to use near-infrared laser excitation. Metal nanoparticles are particularly effective at absorbing near-infrared (NIR) light and converting that light into heat (Alarcon et al. 2015).

Silver nanoparticles have large absorption cross section, and it almost absorbs visible light and produces heat, thereby increasing its temperature. This makes it an

important candidate with regard to plasmonic photothermal therapy (PPTT) (El-Sayed et al. 2006). By controlling the surface functionalization of nanoparticles, they can be tailored to accumulate in tumour cells.

Most photothermal therapy strategies presently use gold nanoparticles due to their superior stability under many different conditions, in biological relevant mediums. Biomolecule conjugated AgNP synthesis, with good stability, is rapidly developing and opening the door to using AgNP in more PPTT strategies (Alarcon et al. 2012, 2013). The superior optical properties of AgNP in comparison to gold make it even more attractive for higher efficiencies of light to heat conversion in PPTT.

8.7 Application of Optical and Photothermal Effect in Biology

Day by day new methods are being introduced based on the optical and photothermal effects for the detection, diagnostics (in vitro and in vivo) and therapy.

8.7.1 *In Vitro Detection and Diagnostics*

In the field of in vitro detection of biomolecules, a new type of ELISA strategy is developed and introduced by Steven's group called plasmonic ELISA. They developed a plasmonic nanosensor with inverse sensitivity via enzyme-guided crystal growth (Rodriguez-Lorenzo et al. 2012). Gold nanostars were used as the nanosensors. Glucose oxidase (GOx) enzyme-linked detection antibody controls the generation of hydrogen peroxide (H_2O_2), which reduces silver ions to atoms. At low concentrations of GOx, conformal coating of silver on the gold nanostar is favoured due to low Ag self-nucleation. It causes a large plasmon peak shift. In contrast, at high loading of GOx, competitive Ag self-nucleation dominates owing to more available H_2O_2 . It reduces the deposition of silver on the gold nanostar, thus generating less peak shift. It therefore provides an inverse graph of spectral shift vs. analyte concentration. In the buffered solution, 10^{-18} g ml^{-1} of a cancer marker prostate-specific antigen (PSA) has been detected with a dynamic range between 10^{-13} and 10^{-18} gml^{-1} .

In another work of Steven's group, catalase enzyme was linked to the immunocomplex through interactions between enzyme-decorated streptavidin and biotinylated secondary antibodies. In the presence of hydrogen peroxide, gold ions are reduced. High concentration of hydrogen peroxide favours the formation of non-aggregated, spherical nanoparticles that give rise to a red solution. When the concentration of hydrogen peroxide decreases, for example, due to the biocatalytic action of the enzyme catalase, aggregates of nanoparticles are formed, and this turns

the solution blue. The range of detection was obtained 10^{-15} – 10^{-19} . This is the highest possible limit of detection (de la Rica and Stevens 2012).

Inspired from this work, many researchers have followed the similar design idea and demonstrated the great potentials of plasmonic ELISA in ultrasensitive detections (Zhao et al. 2016; Xianyu et al. 2014; Peng et al. 2014; Nie et al. 2014; Cecchin et al. 2014; Huang et al. 2016; Tang et al. 2015). For instance, using antibody-tagged gold nanoclusters (AuNCs) to catalyse the decomposition of hydrogen peroxide, Zhao et al. showed sensitive detection of 1×10^{-20} M protein avidin, 7.52×10^{-14} U/ml breast cancer antigen 15-3, 2×10^{-15} mg/ml triiodothyronine and 2.3×10^{-18} mg/ml methamphetamine (Zhao et al. 2016). Using alkaline phosphatase (ALP) linking antibody in combination with iodine-mediated etching of gold nanorods, Zhang et al. exhibited sensitive detection of IgG with a LOD of 100 pg/ml (Zhang et al. 2015).

Based on the chiroplasmonic properties of nanoparticle dimers, Wu et al. (2013) demonstrated the ultralow LOD of 5×10^{-10} ng/ml for PSA. Li et al. fabricated a three-dimensional (3D) hierarchical plasmonic nanostructure. The capture antigen molecules were immobilized on plasmonic gold triangle nanopatterns, while the detection antibody molecules were linked to Raman reporter-labelled gold nanostars. In presence of biomarkers, greatly enhanced electromagnetic field amplified the Raman signal remarkably. In the buffer solution for human immunoglobulin G protein, the SERS immunosensor exhibits a detection range from 0.1 pg/ml to 10 ng/ml with a LOD of 7 fg/ml (Li et al. 2013). The strategy of etching of gold nanorods through the mediation of iodine to generate a plasmonic effect can detect up to 100 pg/ml of IgG (Zhang et al. 2015). In another work for the detection of glucose, gold nanorods were etched by the gradual oxidation in presence of trace concentration of H_2O_2 through the activity of HRP assisted by halide ions by Saa et al. (2014). Silver nanoprism etching-based plasmonic ELISA can detect 100 pg/ml with limit of detection of 4.1 fg/ml (Liang et al. 2015). In the chemical etching, halide ions act as a ligand to reduce the electron potential of the gold species, which enables ferric ions to oxidize the gold nanorods and results in the etching of the gold nanorods. The redox etching leads to a significant decrease of the gold nanorods in length but little change in diameter, which could be attributed to less surface passivation or higher chemical reactivity of the tips of the gold nanorods (Zou et al. 2009).

When gold nanoparticles with about 13 nm in diameter were modified by goat antihuman IgG, the addition of human IgG could change the absorption of colloidal gold solution, and the absorption intensity at 740 nm depended on the amount of human IgG. A dynamic range of 10–500 μ g/3 mL was found (Cao et al. 2009). Rod-shaped Au@PtCu nanostructures show enhanced peroxidase-like activity, and it can replace horse red peroxidase in ELISA. Through this the detection limit reached to 90 picogram per ml (Hu et al. 2014). The enzyme-like activity of NPs can vary by replacing one metal with another. Increasing the percentage of Ag in Au@PtAg decreases the catalytic activity reflected by K_{cat} (Hu et al. 2013b). Additionally Au@PtAg nanorods have a potential antibacterial activity. On increasing the Ag fraction

in the alloy shell up to 80%, the antibacterial activity gradually increases, demonstrating a flexible way to tune this activity. At 80% Ag, the antibacterial activity is better than that of a pure Ag shell (Hu et al. 2013a).

HAuCl_4 salt solution is yellow in colour but changes to orange upon addition of CTAB. Addition of ascorbic acid results in the formation of a colourless solution forming the precursor solution for the plasmonic nanosensor. Irradiation with ionizing radiation results in the formation of coloured dispersions of gold nanoparticle. The colour of gold nanoparticle dispersions (AuNPs) can vary depending on the size of the nanoparticles (Pérez-Juste et al. 2004). This mechanism was utilized by Pushpavanam et al. (2015) for the development of plasmonic nanosensor for dosimetry of therapeutic levels of ionizing radiation. They accomplished this by employing ionizing radiation, in concert with templating lipid surfactant micelles, in order to convert colourless salt solutions of univalent gold ions (Au^1) to maroon-coloured dispersions of plasmonic gold nanoparticles (Pushpavanam et al. 2015).

8.7.2 *In Vivo Monitoring, Detection and Photothermal Effect*

Because of biocompatibility and unique optical properties, gold nanorods (AuNRs) have use in various applications in biomedical research such as imaging, drug and gene delivery and thermal therapy (Weissleder 2001; Huang et al. 2006; Bonoiu et al. 2009; von Maltzahn et al. 2009; Prasad et al. 2017). Jin et al. (2013) showed that negatively charged AuNRs, other than positively charged AuNRs, can penetrate deep into the tumour spheroids and achieve a significant thermal therapeutic benefit. In thermal therapy due to localized surface plasmon resonance, AuNRs convert luminous energy into heat when activated by laser at a specific wavelength (Dickerson et al. 2008). The LSPR maximum can be tuned to near-infrared region by controlling the aspect ratio of AuNRs (Jain et al. 2008). Tri-iodobenzene is used as clinical X-ray contrast agent. Gold has higher absorption than iodine with less bone and tissue interference achieving better contrast with lower X-ray dose. Nanoparticles clear the blood more slowly than iodine agents, permitting longer imaging times. Gold nanoparticles can be used as X-ray contrast agents with properties that overcome some significant limitations of iodine-based agents (Hainfeld et al. 2006).

8.8 Synthesis of Metal NPs

Metal nanoparticles can be synthesized through either of the two approaches, 'top-down' or 'bottom-up'. Top-down approach involves the use of bulk materials and reduces them into nanoparticles by way of physical, chemical or mechanical processes, whereas bottom-up starts from molecules or atoms to obtain nanoparticles.

Top-down approach usually comprises of mechanical energy, high laser energy, lithography, atomization, annealing, arc discharge, laser ablation, electron beam evaporation, radio frequency sputtering, focused ion beam lithography, etc. Bottom-up approach can be divided into gaseous phase, liquid phase, solid phase and biological methods. Chemical vapour deposition and atomic layer deposition come under gaseous phase. Reduction of metal salts, sol-gel processes, templated synthesis and electrodeposition come under the category of liquid-phase methods (Hornyak et al. 2008). Here in this chapter, we will discuss the synthesis as nonbiological and biological synthesis. For the nonbiological method, we will more focus on bottom-up approach because biological synthesis follows only bottom-up approach.

Synthesis via chemical reduction is widely used. It involves different phenomenon/mechanism like reduction, nucleation, growth, etching and some others (Cushing et al. 2004). For any redox reaction, the values of the standard reduction potentials (E_0) determine the pairs of reactants required for successful chemical conversion. It means that the free energy change in the reaction, ΔG_0 , must be negative or what is equivalent to $\Delta E_0 > 0$. For example, in the case of silver, the relatively large electropositive reduction potential of $\text{Ag}^+ \rightarrow \text{Ag}^0$ in water ($E_0 = +0.799$ V, Haynes (2016)) permits the use of several reducing agents, e.g. sodium citrate ($E_0 = -0.180$ V, Li et al. (2013)), sodium borohydride ($E_0 = -0.481$ V, Haynes (2016)), hydrazine ($E_0 = -0.230$ V, Cushing et al. (2004)) and hydroquinone ($E_0 = -0.699$ V, Ullmann (2000); Alarcon et al. (2015)).

Some other commonly used methods are photochemical and electrochemical methods. Direct photoreduction has been established as an important technique for metal NP synthesis, where Mo is formed through the direct excitation of a metal source, normally a salt. Due to the advantage of being free from reducing agents, it has been widely employed in the various mediums including polymer films, glasses, cells, etc. (Sakamoto et al. 2009).

8.8.1 Biological Methods

Biological approach can be classified on the basis of extracellular and intracellular synthesis. Chemical reduction is the main mechanism behind almost all biological methods for the synthesis of nanoparticles. A lot of reducing agents are available in both the intracellular and extracellular environments. Simultaneously a lot of reducing agents are involved in the reduction process. Hence, a biological nanoparticle produced in an intracellular or extracellular environment is the result of many reducing agents. There is a lot of work published on the biological methods of synthesis via bacteria, actinomycetes, algae, fungi, yeasts, viruses, etc. (Mukherjee et al. 2001; Shankar et al. 2004; Gericke and Pinches 2006; Prasad 2014; Prasad et al. 2016).

8.9 Factors Behind Uniformity of NPs

For a tuned optical and photothermal effect, the shape and size of a synthesized nanoparticle must be uniform. A more controlled and regulated process of synthesis yields uniform nanoparticles accordingly. For a controlled and regulated synthetic process, the reduction rate, reaction kinetics and physical parameters are the key factor. Further identification of chemicals which takes part in reaction or affects the reaction or attached to the surface of nanoparticles is necessary for a controlled synthesis process which yields desired uniform nanoparticles in turn to get specific optical or photothermal properties.

The redox potential is a characteristic of the chemical species to undergo an oxidation-reduction reaction. It is a stored energy that has the ability to do work and is measured in volt; thus, the greater the voltage, the greater the ability and propensity to undergo a redox reaction (Harris 2010). The stronger the reducing agent, the faster is the reaction. Mild reducing agent has a great role in achieving desired shape and size of NPs. At many instances, synthesis of bimetallic or tri-metallic NPs is achieved through mild reducing agents. It might be possible that during synthesis of multimetallic NPs, strong reducing agent reduces one metal completely and other metals may not reduce or partially reduce.

Kinetics of a reaction plays a crucial role in the determination of uniformity of the product (NPs). A slow reaction is easy to monitor and control. A slow reaction provides sufficient time to add other ingredients during different steps of a reaction. A very fast reaction can provide non-uniform NPs. Taking silver nucleation as an example, at too much basic condition, the reaction kinetics increases and yields non-uniform AgNPs. When the same reaction is controlled and slowed down by adding dispersing agent, the yield is almost uniform AgNPs with a sharp absorption peak at 400 nm. Kinetics of a reaction is affected by parameters like temperature, pH and concentration of ingredients and presence of poisons, drugs and inhibitors. Catalytic activity of gold nanoparticles is poisoned by sulphur compounds, such as sulphides and sulphites, and inhibited by protecting molecules, such as polyvinyl alcohol (Comotti et al. 2004). There are a variety of types of inhibitors such as irreversible and reversible ones. Reversible inhibition can be further differentiated as competitive, uncompetitive or mixed inhibition, each affecting the Michaelis-Menten constant (K_m) and maximal reaction velocity (V_{max}) in a specific fashion. NaN_3 and Fe^{2+} ions show inhibition behaviours to the oxidase-like activity of Au@Pt NRs (Liu et al. 2011).

Surfactants and some other directional agents are used for the growth of NPs in a shape and aspect ratio. Dispersing agents prevent the NPs from aggregation and allow NPs to grow independently to a uniform shape and size. CTAB is a detergent which acts as both surfactant and dispersing agent. Seed-mediated growth is a good approach for the synthesis of uniform-shaped and uniform-sized NPs. Here seed acts as nuclei which grow further. The directional agent directs the growth of a seed to a specific shape. Similarly size and aspect ratio are determined by other constituents of the reaction such as Ag^+ in case of AuNRs. The gold nanorods are synthesized

through seed-mediated and surfactant-assisted method. The seed which is a ~ 1.5 nm diameter gold nanoparticle is synthesized by mixing aqueous solutions of hexadecyltrimethylammonium bromide (CTAB), hydrogen tetrachloroaurate (III) hydrate and sodium borohydride in a specific ratio (Orendorff and Murphy 2006). These fresh gold seeds are then added to a growth solution of concentrated CTAB, silver nitrate, hydrogen tetrachloroaurate (III) hydrate and ascorbic acid (Nikoobakht and El-Sayed 2003). Ascorbic acid is a weak/mild reducing agent that induces heterogeneous gold deposition at the surface of the seed particles (Murphy et al. 2005). Anisotropic nanorod growth results from facet-selective gold deposition promoted by the silver ions, which get adsorbed on the gold surfaces by an underpotential deposition (UPD) mechanism as elucidated by Liu and Guyot-Sionnest (Liu and Guyot-Sionnest 2005). The nanorod aspect ratio can be increased to a certain extent, up to 4.5, by increasing the silver concentration (Nikoobakht and El-Sayed 2003), and the absence of Ag^+ from the reactions leads to only a very low yield of Au nanorods. CTAB coats the nanorod surface as a bilayer that prevents aggregation (Nikoobakht and El-Sayed 2001). CTAB is also believed to aid nanorod growth by facet-sensitive surface adsorption (Smith and Korgel 2008). The synthesis process needs specific ingredients with purity, controlled and regulated reaction for the yield of uniform gold nanorods and reproducible results. So a controlled and regulated synthesis procedure with known ingredients and reaction mechanism results in the yield of uniform NPs and reproducible results.

8.10 How to Get Uniform Biological NPs

To get uniform-shaped and uniform-sized biological NPs, the ingredients, reducing agents, reaction mechanism and all other factors which can promote or inhibit the synthesis must be known. Usually in an extracellular or intracellular environment, several reducing agents are present in different concentrations from mild to strong. The pH of the cellular environment is controlled by the cell and cannot be altered too much. Inhibitors may also be present in the biological media which can inhibit fully or partially the synthesis process. All the above-mentioned factors can vary in concentrations with respect to growth rate or growth conditions and with change in strains of bacteria or fungus. This is applicable to both types of extracts whether it is intracellular or extracellular.

Mukherjee et al. (2012) tried to find out the mechanism of biosynthesis of gold nanoparticle. It has been found that low (10–15 kDa) and high molecular weight protein molecules (100–200 kDa), amino acids, phenolic compounds (wedelolactone, desmethylwedelolactone, stigmasterol, etc.), starch, polysaccharides, alkaloids, alcoholic compounds, vitamins, enzymes, etc. present in *Eclipta alba* leaf help in the formation and stabilization of gold nanoparticles (AuNPs) (Shukla et al. 2008; Wilson et al. 1986; Jadhav et al. 2009; Chaudhary et al. 2011; Xie et al. 2007; Zhu et al. 2008; Iravani 2011; Bhargava et al. 2005; Sarma and Chattopadhyay 2004). There may be several types of molecules present in a biological extract.

A few can act as reductant and others may act as stabilizing agent. Many biologically synthesized NPs show good stability at different pH conditions. This is due to many naturally present stabilizers which form mono- or multilayer over the surface of NPs. Some compound acts as directional agents for growth process. The presence of different directional agents causes the yield of different-shaped NPs from the same synthesis method with different concentrations. Because of many directional agents in the same reaction, the uniformity is not maintained.

Ascorbic acid is a naturally occurring mild reducing agent widely used for the synthesis of NPs. CTAB is the surfactant, directional agent, dispersing agent and stabilizer for NPs. It is widely used for the synthesis of AuNRs. A few reports have been published about the biological synthesis of AuNRs (Parial et al. 2012). Till date we don't have any biological equivalent of CTAB which can replace it. For defined NP synthesis, if the ingredients from biological origin such as reducing agents, surfactants, directional agents, inhibitors and stabilizers are known, then green NPs can be produced in vitro. Unknown biological compounds involved in the synthesis of NPs can be known through different characterization techniques like HPLC, gas chromatography, NMR, etc.

The spectra of nanoparticles provide information about the uniformity in terms of shape and size. A sharp-pointed peak in spectra denotes specific information about nanoparticle. A broad peak denotes nanoparticles of different shapes and sizes. Spherical nanoparticles show a single peak, while nanorods show two peaks, one longitudinal and the other transverse. It also provides information of other chemicals present in the sample. For example, ascorbic acid which is widely used in the synthesis of nanoparticles has a specific absorbance peak at 265 nm. A typical spectrum of silver nanoparticles is shown in Fig. 8.4.

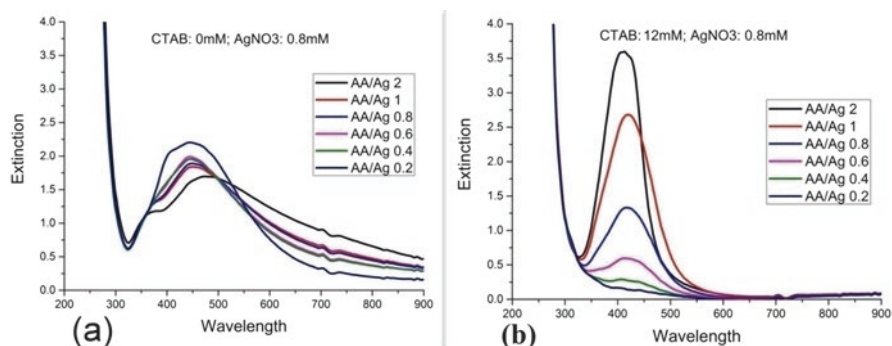


Fig. 8.4 Spectra of silver nanoparticles synthesized via ascorbic acid as reducing agent and CTAB as dispersing agent. Silver concentration is constant. Here CTAB controls the reaction rate. (a) In absence of dispersing agent CTAB, the reaction is very fast that leads in non-uniform silver nanoparticles having wide distribution in their shape and size. (b) At high concentration of CTAB, the reaction rate is slow and thus controlled. The shape is uniform. With increase in reducing agent AA, more silver reduced and results in the increase of size which is reflected from the increasing extinction

8.11 Conclusion

To obtain biological nanoparticles with defined optical and photothermal properties, uniformity in shape and size is a must. Uniformity can be achieved by understanding the mechanism of reaction, and one should have a control over it. Identification of enzymes, reducing agents, dispersing agents, directional agents and stabilizers of biological origin is necessary in order to synthesize uniform nanoparticles *in vitro*. *In vitro* synthesis of nanoparticles has always better control over *in vivo* synthesis. Additionally the purification of nanoparticles is easy and saves time.

References

- Abalde-Cela S, Aldeanueva-Potel P, Mateo-Mateo C, Rodríguez-Lorenzo L, Alvarez-Puebla RA, Liz-Marzán LM (2010) Surface-enhanced Raman scattering biomedical applications of plasmonic colloidal particles. *J R Soc Interface* 7(Suppl 4):S435–S450
- Alarcon EI, Udekwu K, Skog M, Pacioni NL, Stamplecoskie KG, Gonzalez-Bejar M, Poliseti N, Wickham A, Richter-Dahlfors A, Griffith M, Scaiano JC (2012) The biocompatibility and antibacterial properties of collagen-stabilized, photochemically prepared silver nanoparticles. *Biomaterials* 33(19):4947–4956. <https://doi.org/10.1016/j.biomaterials.2012.03.033>
- Alarcon EI, Bueno-Alejo CJ, Noel CW, Stamplecoskie KG, Pacioni NL, Poblete H, Scaiano JC (2013) Human serum albumin as protecting agent of silver nanoparticles: role of the protein conformation and amine groups in the nanoparticle stabilization. *J Nanopart Res* 15(1):1374. <https://doi.org/10.1007/s11051-012-1374-7>
- Alarcon E, Griffith M, Udekwu KI (2015) Silver nanoparticle applications: in the fabrication and design of medical and biosensing devices. Springer, Cham
- Bhargava SK, Booth JM, Agrawal S, Coloe P, Kar G (2005) Gold nanoparticle formation during bromoaurate reduction by amino acids. *Langmuir* 21(13):5949–5956
- Bonoiu AC, Mahajan SD, Ding H, Roy I, Yong K-T, Kumar R, Hu R, Bergery EJ, Schwartz SA, Prasad PN (2009) Nanotechnology approach for drug addiction therapy: gene silencing using delivery of gold nanorod-siRNA nanoplex in dopaminergic neurons. *Proc Natl Acad Sci* 106(14):5546–5550
- Campion A, Kambhampati P (1998) Surface-enhanced Raman scattering. *Chem Soc Rev* 27(4):241–250
- Cao QH, Yuan H, Cai RX (2009) Homogeneous detection of human IgG by gold nanoparticle probes. *J Wuhan Univ Technol* 24(5):772–775. <https://doi.org/10.1007/s11595-009-5772-3>
- Cecchin D, de la Rica R, Bain RES, Finnis MW, Stevens MM, Battaglia G (2014) Plasmonic ELISA for the detection of gp120 at ultralow concentrations with the naked eye. *Nanoscale* 6(16):9559–9562. <https://doi.org/10.1039/c3nr06167a>
- Chaudhary H, Dhuna V, Singh J, Kamboj SS, Seshadri S (2011) Evaluation of hydro-alcoholic extract of *Eclipta alba* for its anticancer potential: an *in vitro* study. *J Ethnopharmacol* 136(2):363–367
- Choi CJ, Xu Z, Wu H-Y, Liu GL, Cunningham BT (2010) Surface-enhanced Raman nanodomains. *Nanotechnology* 21(41):415301
- Comotti M, Della Pina C, Matarrese R, Rossi M (2004) The catalytic activity of “naked” gold particles. *Angew Chem Int Ed Eng* 43(43):5812–5815. <https://doi.org/10.1002/anie.200460446>
- Cushing BL, Kolesnichenko VL, O'Connor CJ (2004) Recent advances in the liquid-phase syntheses of inorganic nanoparticles. *Chem Rev* 104(9):3893–3946. <https://doi.org/10.1021/cr030027b>

- Dickerson EB, Dreaden EC, Huang X, El-Sayed IH, Chu H, Pushpanketh S, McDonald JF, El-Sayed MA (2008) Gold nanorod assisted near-infrared plasmonic photothermal therapy (PPTT) of squamous cell carcinoma in mice. *Cancer Lett* 269(1):57–66
- El-Sayed IH, Huang X, El-Sayed MA (2006) Selective laser photo-thermal therapy of epithelial carcinoma using anti-EGFR antibody conjugated gold nanoparticles. *Cancer Lett* 239(1):129–135. <https://doi.org/10.1016/j.canlet.2005.07.035>
- EwenáSmith W (2002) Selective functionalisation of TNT for sensitive detection by SERRS. *Chem Commun* 6:580–581
- Fano U (1941) The theory of anomalous diffraction gratings and of quasi-stationary waves on metallic surfaces (Sommerfeld's Waves). *J Opt Soc Am* 31(3):213–222. <https://doi.org/10.1364/JOSA.31.000213>
- Faulds K, Littleford RE, Graham D, Dent G, Smith WE (2004) Comparison of surface-enhanced resonance Raman scattering from unaggregated and aggregated nanoparticles. *Anal Chem* 76(3):592–598
- Fleischmann M, Hendra PJ, McQuillan AJ (1974) Raman spectra of pyridine adsorbed at a silver electrode. *Chem Phys Lett* 26(2):163–166
- Fu Y, Wang J, Zhang D (2012) Modelling at nanoscale. Plasmonics – principles and applications. Intech, Rijeka. doi: 40334. <https://www.intechopen.com/books/plasmonics-principles-and-applications/modelling-at-nanoscale>
- Gericke M, Pinches A (2006) Microbial production of gold nanoparticles. *Gold Bull* 39(1):22–28
- Graham D, Goodacre R (2008) Chemical and bioanalytical applications of surface enhanced Raman scattering spectroscopy. *Chem Soc Rev* 37(5):883–884
- Hainfeld JF, Slatkin DN, Focella TM, Smilowitz HM (2006) Gold nanoparticles: a new X-ray contrast agent. *Brit J Radiol* 79(939):248–253. <https://doi.org/10.1259/Bjpr/13169882>
- Harris DC (2010) Quantitative chemical analysis. W. H. Freeman and Company, New York
- Hartland GV (2011) Optical studies of dynamics in noble metal nanostructures. *Chem Rev* 111(6):3858–3887. <https://doi.org/10.1021/cr1002547>
- Haynes WM (2016) CRC handbook of chemistry and physics, 97th edn. CRC Press
- Hornyak GL, Dutta J, Tibbals HF, Rao A (2008) Introduction to nanoscience. CRC Press, Boca Raton
- Hu X, Zhao Y, Hu Z, Saran A, Hou S, Wen T, Liu W, Ji Y, Jiang X, Wu X (2013a) Gold nanorods core/AgPt alloy nanodots shell: a novel potent antibacterial nanostructure. *Nano Res* 6(11):822–835
- Hu XN, Saran A, Hou S, Wen T, Ji YL, Liu WQ, Zhang H, He WW, Yin JJ, Wu XC (2013b) Au@PtAg core/shell nanorods: tailoring enzyme-like activities via alloying. *RSC Adv* 3(17):6095–6105. <https://doi.org/10.1039/C3ra23215h>
- Hu X, Saran A, Hou S, Wen T, Ji Y, Liu W, Zhang H, Wu X (2014) Rod-shaped Au@PtCu nanostructures with enhanced peroxidase-like activity and their ELISA application. *Chin Sci Bull* 59(21):2588–2596. <https://doi.org/10.1007/s11434-014-0316-4>
- Huang X, El-Sayed IH, Qian W, El-Sayed MA (2006) Cancer cell imaging and photothermal therapy in the near-infrared region by using gold nanorods. *J Am Chem Soc* 128(6):2115–2120
- Huang XL, Chen R, Xu HY, Lai WH, Xiong YH (2016) Nanospherical brush as catalase container for enhancing the detection sensitivity of competitive plasmonic ELISA. *Anal Chem* 88(3):1951–1958. <https://doi.org/10.1021/acs.analchem.5b04518>
- Hvolbæk B, Janssens TVW, Clausen BS, Falsig H, Christensen CH, Nørskov JK (2007) Catalytic activity of Au nanoparticles. *Nano Today* 2(4):14–18. [https://doi.org/10.1016/s1748-0132\(07\)70113-5](https://doi.org/10.1016/s1748-0132(07)70113-5)
- Iravani S (2011) Green synthesis of metal nanoparticles using plants. *Green Chem* 13(10):2638–2650
- Jadhav V, Thorat R, Kadam V, Salaskar K (2009) Chemical composition, pharmacological activities of *Eclipta alba*. *J Pharm Res* 2(8):1229–1231
- Jain PK, Huang X, El-Sayed IH, El-Sayed MA (2008) Noble metals on the nanoscale: optical and photothermal properties and some applications in imaging, sensing, biology, and medicine. *Acc Chem Res* 41(12):1578–1586
- Jin S, Ma X, Ma H, Zheng K, Liu J, Hou S, Meng J, Wang PC, Wu X, Liang X-J (2013) Surface chemistry-mediated penetration and gold nanorod thermotherapy in multicellular tumor spheroids. *Nanoscale* 5(1):143–146

- Jonsson U, Fagerstam L, Ivarsson B, Johnsson B, Karlsson R, Lundh K, Lofas S, Persson B, Roos H, Ronnberg I et al (1991) Real-time biospecific interaction analysis using surface plasmon resonance and a sensor chip technology. *BioTechniques* 11(5):620–627
- Kelly KL, Coronado E, Zhao LL, Schatz GC (2003) The optical properties of metal nanoparticles: the influence of size, shape, and dielectric environment. *J Phys Chem B* 107(3):668–677. <https://doi.org/10.1021/jp026731y>
- Khanna S, Jena P (1995) Atomic clusters: building blocks for a class of solids. *Phys Rev B* 51(19):13705
- Kretschmann E, Raether H (1968) Radiative decay of nonradiative surface plasmons excited by light. *Z Naturforsch A* 23:2135. doi:citeulike-article-id:3901347
- Li M, Cushing SK, Zhang J, Suri S, Evans R, Petros WP, Gibson LF, Ma D, Liu Y, Wu N (2013) Three-dimensional hierarchical plasmonic nano-architecture enhanced surface-enhanced Raman scattering immunosensor for cancer biomarker detection in blood plasma. *ACS Nano* 7(6):4967–4976. <https://doi.org/10.1021/nn4018284>
- Liang JJ, Yao CZ, Li XQ, Wu Z, Huang CH, Fu QQ, Lan CF, Cao DL, Tang Y (2015) Silver nanoprisms etching-based plasmonic ELISA for the high sensitive detection of prostate-specific antigen. *Biosens Bioelectron* 69:128–134. <https://doi.org/10.1016/j.bios.2015.02.026>
- Liedberg B, Nylander C, Lunström I (1983) Surface plasmon resonance for gas detection and biosensing. *Sensors Actuators* 4:299–304. [https://doi.org/10.1016/0250-6874\(83\)85036-7](https://doi.org/10.1016/0250-6874(83)85036-7)
- Liu M, Guyot-Sionnest P (2005) Mechanism of silver(I)-assisted growth of gold nanorods and bipyramids. *J Phys Chem B* 109(47):22192–22200. <https://doi.org/10.1021/jp054808n>
- Liu JB, Hu XN, Hou S, Wen T, Liu WQ, Zhu X, Wu XC (2011) Screening of inhibitors for oxidase mimics of Au@Pt nanorods by catalytic oxidation of OPD. *Chem Commun* 47(39):10981–10983. <https://doi.org/10.1039/c1cc14346h>
- von Maltzahn G, Park J-H, Agrawal A, Bandaru NK, Das SK, Sailor MJ, Bhatia SN (2009) Computationally guided photothermal tumor therapy using long-circulating gold nanorod antennas. *Cancer Res* 69(9):3892–3900
- McNay G, Eustace D, Smith WE, Faulds K, Graham D (2011) Surface-enhanced Raman scattering (SERS) and surface-enhanced resonance Raman scattering (SERRS): a review of applications. *Appl Spectrosc* 65(8):825–837
- Motz JT, Fitzmaurice M, Miller A, Gandhi SJ, Haka AS, Galindo LH, Dasari RR, Kramer JR, Feld MS (2006) In vivo Raman spectral pathology of human atherosclerosis and vulnerable plaque. *J Biomed Opt* 11(2):021003–021003. -021009
- Mukherjee P, Ahmad A, Mandal D, Senapati S, Sainkar SR, Khan MI, Ramani R, Parischa R, Ajayakumar PV, Alam M, Sastry M, Kumar R (2001) Bioreduction of AuCl₄(–) ions by the fungus, *Verticillium* sp. and surface trapping of the gold nanoparticles formed. *Angew Chem Int Ed Eng* 40(19):3585–3588
- Mukherjee S, Sushma V, Patra S, Barui AK, Bhadra MP, Sreedhar B, Patra CR (2012) Green chemistry approach for the synthesis and stabilization of biocompatible gold nanoparticles and their potential applications in cancer therapy. *Nanotechnology* 23(45):455103
- Murphy CJ, Sau TK, Gole AM, Orendorff CJ, Gao J, Gou L, Hunyadi SE, Li T (2005) Anisotropic metal nanoparticles: synthesis, assembly, and optical applications. *J Phys Chem B* 109(29):13857–13870. <https://doi.org/10.1021/jp0516846>
- Nie XM, Huang R, Dong CX, Tang LJ, Gui R, Jiang JH (2014) Plasmonic ELISA for the ultra-sensitive detection of *Treponema pallidum*. *Biosens Bioelectron* 58:314–319. <https://doi.org/10.1016/j.bios.2014.03.007>
- Nikoobakht B, El-Sayed MA (2001) Evidence for bilayer assembly of cationic surfactants on the surface of gold nanorods. *Langmuir* 17(20):6368–6374. <https://doi.org/10.1021/la010530o>
- Nikoobakht B, El-Sayed MA (2003) Preparation and growth mechanism of gold nanorods (NRs) using seed-mediated growth method. *Chem Mater* 15(10):1957–1962. <https://doi.org/10.1021/cm020732l>
- Oh YJ, Park SG, Kang MH, Choi JH, Nam Y, Jeong KH (2011) Beyond the SERS: Raman enhancement of small molecules using nanofluidic channels with localized surface plasmon resonance. *Small (Weinheim an der Bergstrasse, Germany)* 7(2):184–188

- Orendorff CJ, Murphy CJ (2006) Quantitation of metal content in the silver-assisted growth of gold nanorods. *J Phys Chem B* 110(9):3990–3994. <https://doi.org/10.1021/jp0570972>
- Otto A (1968) Excitation of nonradiative surface plasma waves in silver by the method of frustrated total reflection. *Zeitschrift für Physik A Hadrons and nuclei* 216(4):398–410. <https://doi.org/10.1007/bf01391532>
- Parial D, Patra HK, Roychoudhury P, Dasgupta AK, Pal R (2012) Gold nanorod production by cyanobacteria—a green chemistry approach. *J Appl Phycol* 24(1):55–60. <https://doi.org/10.1007/s10811-010-9645-0>
- Peng CF, Duan XH, Khamba GW, Xie ZJ (2014) Highly sensitive “signal on” plasmonic ELISA for small molecules by the naked eye. *Anal Methods-Uk* 6(24):9616–9621. <https://doi.org/10.1039/c4ay01993h>
- Pérez-Juste J, Liz-Marzan L, Carnie S, Chan DY, Mulvaney P (2004) Electric-field-directed growth of gold nanorods in aqueous surfactant solutions. *Adv Funct Mater* 14(6):571–579
- Poole CP, Owens FJ (2003) Introduction to nanotechnology. Wiley, Hoboken
- Prasad R (2014) Synthesis of silver nanoparticles in photosynthetic plants. *J Nanoparticles*, Article ID 963961, <https://doi.org/10.1155/2014/963961>
- Prasad R, Pandey R, Barman I (2016) Engineering tailored nanoparticles with microbes: quo vadis. *WIREs Nanomedicine Nanobiotechnology* 8:316–330. <https://doi.org/10.1002/wnan.1363>
- Prasad R, Bhattacharyya A, Nguyen QD (2017) Nanotechnology in sustainable agriculture: recent developments, challenges, and perspectives. *Front Microbiol* 8:1014. <https://doi.org/10.3389/fmicb.2017.01014>
- Pushpavanam K, Narayanan E, Chang J, Sapareto S, Rege K (2015) A colorimetric plasmonic nanosensor for dosimetry of therapeutic levels of ionizing radiation. *ACS Nano* 9(12):11540–11550. <https://doi.org/10.1021/acs.nano.5b05113>
- Qian X-M, Nie S (2008) Single-molecule and single-nanoparticle SERS: from fundamental mechanisms to biomedical applications. *Chem Soc Rev* 37(5):912–920
- Raman C, Krishnan K (1998) A new type of secondary radiation (reprinted from nature, vol 121, pg 501–502, 1928). *Curr Sci* 74(4):381–381
- Rao B, Khanna S, Jena P (1999) Designing new materials using atomic clusters. *J Clust Sci* 10(4):477–491
- Rayleigh L (1907) On the dynamical theory of gratings. *Proc R Soc London Ser A* 79(532):399–416. <https://doi.org/10.1098/rspa.1907.0051>
- de la Rica R, Stevens MM (2012) Plasmonic ELISA for the ultrasensitive detection of disease biomarkers with the naked eye. *Nat Nanotechnol* 7(12):821–824. <https://doi.org/10.1038/nnano.2012.186>
- de la Rica R, Stevens MM (2013) Plasmonic ELISA for the detection of analytes at ultralow concentrations with the naked eye. *Nat Protoc* 8(9):1759–1764. <https://doi.org/10.1038/nprot.2013.085>
- Rodriguez-Lorenzo L, de la Rica R, Alvarez-Puebla RA, Liz-Marzan LM, Stevens MM (2012) Plasmonic nanosensors with inverse sensitivity by means of enzyme-guided crystal growth. *Nat Mater* 11(7):604–607. <https://doi.org/10.1038/Nmat3337>
- Saa L, Coronado-Puchau M, Pavlov V, Liz-Marzan LM (2014) Enzymatic etching of gold nanorods by horseradish peroxidase and application to blood glucose detection. *Nanoscale* 6(13):7405–7409. <https://doi.org/10.1039/C4nr01323a>
- Sakamoto M, Fujistuka M, Majima T (2009) Light as a construction tool of metal nanoparticles: synthesis and mechanism. *J Photochem Photobiol C: Photochem Rev* 10(1):33–56. <https://doi.org/10.1016/j.jphotochemrev.2008.11.002>
- Sarma TK, Chattopadhyay A (2004) Starch-mediated shape-selective synthesis of Au nanoparticles with tunable longitudinal plasmon resonance. *Langmuir* 20(9):3520–3524
- Schatz GC, Van Duyn RP (2002) Electromagnetic mechanism of surface-enhanced spectroscopy. *Handbook of vibrational spectroscopy*. Wiley, Chichester. <http://onlinelibrary.wiley.com/book/10.1002/0470027320>

- Shankar SS, Rai A, Ankamwar B, Singh A, Ahmad A, Sastry M (2004) Biological synthesis of triangular gold nanoprisms. *Nat Mater* 3(7):482–488. <https://doi.org/10.1038/nmat1152>
- Shukla R, Nune SK, Chanda N, Katti K, Mekapothula S, Kulkarni RR, Welshons WV, Kannan R, Katti KV (2008) Soybeans as a phytochemical reservoir for the production and stabilization of biocompatible gold nanoparticles. *Small* (Weinheim an der Bergstrasse, Germany) 4(9):1425–1436. <https://doi.org/10.1002/sml.200800525>
- Siddhanta S, Paidi SK, Bushley K, Prasad R, Barman I (2017) Exploring morphological and biochemical linkages in fungal growth with label-free light sheet microscopy and Raman spectroscopy. *ChemPhysChem* 18(1):72–78
- Smith DK, Korgel BA (2008) The importance of the CTAB surfactant on the colloidal seed-mediated synthesis of gold nanorods. *Langmuir* 24(3):644–649. <https://doi.org/10.1021/La703625a>
- Stamplecoskie KG, Scaiano JC (2010) Light emitting diode irradiation can control the morphology and optical properties of silver nanoparticles. *J Am Chem Soc* 132(6):1825–182+. <https://doi.org/10.1021/ja910010b>
- Tang Y, Zhang W, Liu J, Zhang L, Huang W, Huo FW, Tian DB (2015) A plasmonic nanosensor for lipase activity based on enzyme-controlled gold nanoparticles growth in situ. *Nanoscale* 7(14):6039–6044. <https://doi.org/10.1039/c4nr07579j>
- Turro NJ, Ramamurthy V, Scaiano JC (2012) Modern molecular photochemistry of organic molecules. Wiley Online Library
- Ullmann F (2000) Ullmann's encyclopedia of industrial chemistry. Wiley. http://onlinelibrary.wiley.com/doi/10.1002/14356007.a27_443/abstract
- Weissleder R (2001) A clearer vision for in vivo imaging. *Nat Biotechnol* 19(4):316–316
- Wilson KA, Rightmire BR, Chen JC, Tan-Wilson AL (1986) Differential proteolysis of glycinin and β -conglycinin polypeptides during soybean germination and seedling growth. *Plant Physiol* 82(1):71–76
- Wolf EL (2015) Nanophysics and nanotechnology: an introduction to modern concepts in nanoscience. Wiley
- Wood RW (1902) XLII. On a remarkable case of uneven distribution of light in a diffraction grating spectrum. *Philos Mag Ser 6* 4(21):396–402. <https://doi.org/10.1080/14786440209462857>
- Wood RW (1912) XXVII. Diffraction gratings with controlled groove form and abnormal distribution of intensity. *Philos Mag Ser 6* 23(134):310–317. <https://doi.org/10.1080/14786440208637224>
- Wu X, Xu L, Liu L, Ma W, Yin H, Kuang H, Wang L, Xu C, Kotov NA (2013) Unexpected chirality of nanoparticle dimers and ultrasensitive chiroplasmonic bioanalysis. *J Am Chem Soc* 135(49):18629–18636. <https://doi.org/10.1021/ja4095445>
- Xianyu YL, Wang Z, Jiang XY (2014) A plasmonic nanosensor for immunoassay via enzyme-triggered click chemistry. *ACS Nano* 8(12):12741–12747. <https://doi.org/10.1021/nn505857g>
- Xie J, Lee JY, Wang DI, Ting YP (2007) Identification of active biomolecules in the high-yield synthesis of single-crystalline gold nanoplates in algal solutions. *Small* (Weinheim an der Bergstrasse, Germany) 3(4):672–682
- Zhang ZY, Chen ZP, Wang SS, Cheng FB, Chen LX (2015) Iodine-mediated etching of gold nanorods for plasmonic ELISA based on colorimetric detection of alkaline phosphatase. *ACS Appl Mater Interfaces* 7(50):27639–27645. <https://doi.org/10.1021/acsami.5b07344>
- Zhao Q, Huang HW, Zhang LY, Wang LQ, Zeng YL, Xia XD, Liu FP, Chen Y (2016) Strategy to fabricate naked-eye readout ultrasensitive plasmonic nanosensor based on enzyme mimetic gold nanoclusters. *Anal Chem* 88(2):1412–1418. <https://doi.org/10.1021/acs.analchem.5b04089>
- Zhu X, Yang Q, Huang J, Suzuki I, Li G (2008) Colorimetric study of the interaction between gold nanoparticles and a series of amino acids. *J Nanosci Nanotechnol* 8(1):353–357
- Zou R, Guo X, Yang J, Li D, Peng F, Zhang L, Wang H, Yu H (2009) Selective etching of gold nanorods by ferric chloride at room temperature. *Cryst Eng Comm* 11(12):2797. <https://doi.org/10.1039/b911902g>